

Structural transformation of liquid tellurium at high pressures and temperatures

Nobumasa Funamori* and Kazuhiko Tsuji

Department of Physics, Keio University, Yokohama 223-8522, Japan

(Received 6 August 2001; published 4 December 2001)

We have developed synchrotron x-ray-diffraction techniques for studying the structure of liquids at high pressures and high temperatures and have applied them to measuring structural transformation of liquid Te up to 22 GPa. The nearest-neighbor distance of liquid Te, which is 2.9–3.0 Å and already larger than 2.8 Å of crystalline Te at 0 GPa, further increases with pressure to 3.1 Å at 6 GPa in spite of the volume contraction, and then decreases gradually at higher pressures. The anomalous expansion of the nearest-neighbor distance can be attributed to the increase in coordination number from 2–3 at 0 GPa to 4 at 6 GPa and the resultant weakening of the covalent bond. The coordination number further increases with pressure and approaches to 14, i.e., the number for a closely packed simple-liquid structure, at 22 GPa. However, the effect of the increase in coordination number on the nearest-neighbor distance is much smaller in a dense metallic state at high pressures than in a sparse covalent state at low pressures.

DOI: 10.1103/PhysRevB.65.014105

PACS number(s): 62.50.+p, 61.10.-i, 61.25.-f

I. INTRODUCTION

The pure substances consisting of covalently bonded atoms such as chalcogens and halogens have several distinct bonds in each crystal structure. As each bond has different length and strength, these crystals show anisotropic contraction under pressure.¹ They also show the pressure-induced phase transitions accompanied by discontinuous increases in coordination number and the nearest-neighbor distance r_1 .^{2–4} Structural measurements have revealed that covalent liquids also show (microscopically) anisotropic contraction under pressure.⁵ However, continuous transitions have been suggested to occur at different pressures from their crystalline counterparts.^{6–9} This may be attributed to the fact that liquid structures are free from periodicity and are allowed to have plural local structures to minimize free energy. Because of technical difficulties, however, no experimental studies on liquid structures have been made at high enough pressures, in contrast with the case for crystals.¹⁰ The maximum pressure was limited to about 8 GPa in previous work.^{5,9,11–13} To extend the pressure limit, we have developed experimental techniques by combining synchrotron x-ray diffraction with a double-stage high-pressure and high-temperature apparatus. Here, we report measurements of liquid structures at extremely high pressures to over 20 GPa, which make it possible to discuss the whole transformation from a highly covalent complex-liquid state to a closely packed simple-liquid state.

The chalcogen elements Se and Te are among the most interesting materials to be studied. The two elements, both in solid and liquid states, have a similar sequence of high-pressure transitions with lower transition pressures for Te.^{2,3,8,14–19} The metallization of liquid Se (*l*-Se) occurs at 4 GPa just above melting temperatures,⁸ while *l*-Te is metallic even at 0 GPa and the metallization occurs in its supercooled-liquid state.^{14–17} Numerous experimental and theoretical studies on these elements at 0 GPa have suggested that semiconducting liquids consist of long chains of covalently bonded atoms, whereas metallic liquids consist of entangled broken chains with long and short covalent

bonds.^{14,16,17,20–22} In *l*-Te, another transition occurs at 5 GPa just above melting temperatures.^{7,12,23} The nature of this transition has not been clarified yet. The transition may take place also in *l*-Se but at pressures beyond experimental limits. Therefore Te is more suitable for the search on pressure-induced structural changes within a limited pressure range. We report structural transformation of *l*-Te up to 22 GPa, which is equivalent to 100–120 GPa in Se,^{2,3} with detailed comparison with transitions of crystalline Te (*c*-Te).

II. EXPERIMENTAL AND ANALYTICAL PROCEDURES

High-pressure and high-temperature x-ray-diffraction experiments on *l*-Te were carried out, by utilizing the SPEED-1500 system²⁴ installed at the SPring-8 synchrotron facility (Japan) and the MAX90 system¹³ at the PF synchrotron facility (Japan). In conventional SPEED-1500 experiments, diffracted x rays of crystals are measured at a fixed diffraction angle 2θ of about 5° because of the severe restriction due to the double-stage-compression geometry of the system. In the present study, the size and shape of both anvils and sample assemblies (Fig. 1) were designed so as to make it possible to measure diffracted x rays of liquids at a wide range of 2θ between 3 and 15° without any significant changes in x-ray absorption. The double-stage compression of SPEED-1500 has extended the pressure limit of x-ray diffraction on liquids nearly three times. The SPEED-1500 system was used for the measurements at 6, 12, 18, and 22 GPa. The MAX90 system with single-stage compression was used for lower-pressure measurements at 3 and 4 GPa. Experimental techniques used in the two systems were similar except for the mechanism of high-pressure generation.

In the present study, a powdered mixture of *c*-Te and NaCl was placed in a NaCl capsule as a starting material (Fig. 1). This sample assemblage prevented leakage and degeneration of *l*-Te during measurements, as confirmed from time-independent x-ray-diffraction profiles. Measurements were made at temperatures about 50 K above the melting point of each pressure.⁷ Temperature was estimated from the phase diagram of Te,⁷ assuming proportionality between

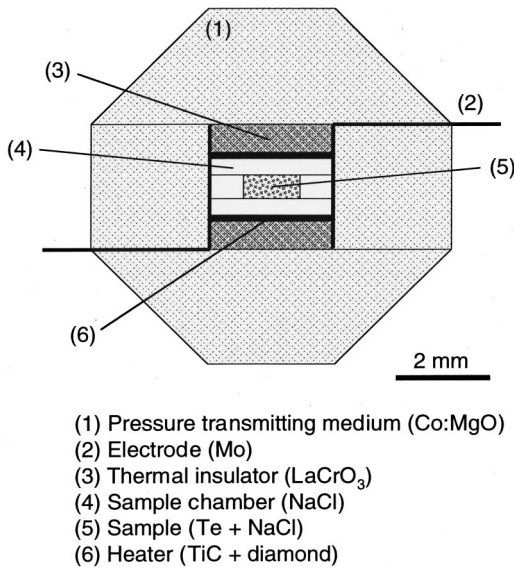


FIG. 1. Cross section of the sample assembly used in the highest-pressure measurement (Ref. 24).

temperature and supplied electrical power for heating. Pressure was calculated based on thus estimated temperature and the unit-cell volume of NaCl, measured by x-ray diffraction, using an equation of state for NaCl.²⁵ Pressure uncertainty is estimated to be less than ± 1 GPa even in the highest-pressure measurement at 22 GPa, assuming temperature uncertainty of up to ± 200 K.

Energy-dispersive diffraction profiles were measured at 6–9 different 2θ between 3 and 15° with white x rays of 60–120 keV (i.e., $1.6 \leq Q = 4\pi \sin \theta/\lambda = 4\pi \sin \theta E/12.398 \leq 16 \text{ \AA}^{-1}$, where λ and E are wavelength and energy of x ray) using a pure-Ge solid-state detector. An example of diffraction profiles of *l*-Te at 22 GPa measured at various 2θ is shown in Fig. 2. A fine x-ray optical system, together with low divergence of synchrotron x rays, prevented the profiles from the contamination with unfavorable diffraction of surrounding materials as shown in Fig. 2. Analytical procedures described in a previous paper¹¹ have been improved and used in the present study. The procedures are briefly summarized as follows. Static structure factor $S(Q)$ for each pressure was obtained by combining all the profiles after the corrections for energy distribution of incident x rays, atomic scattering factor of the specimen, absorption and incoherent scattering by the specimen and pressure-transmitting mediums. The wide energy range of synchrotron x rays was suitable for combining the profiles. Further minor corrections for $S(Q)$ were made so that $S(Q)$ and pair distribution function $g(r)$, which is related with $S(Q)$ via Fourier transformation,²⁶ are consistent with each other and are physically appropriate. The corrections were based on (i) $S(Q)$ smoothly approaches to $\rho \kappa_T kT$ (close to 0) at $Q=0$, where ρ , κ_T , k , and T are number density, isothermal compressibility, Boltzmann constant, and temperature, respectively, (ii) $g(r)$ is 0 inside the first coordination shell (i.e., $r \leq 2 \text{ \AA}$ for *l*-Te), and (iii) integration of $(1/2\pi^2)[1 - S(Q)]Q^2 dQ$ at $0 < Q < \infty$ equals to ρ . The quality of measured $S(Q)$ of the present study (Fig. 3) seems to be comparable to that of previous work at 0

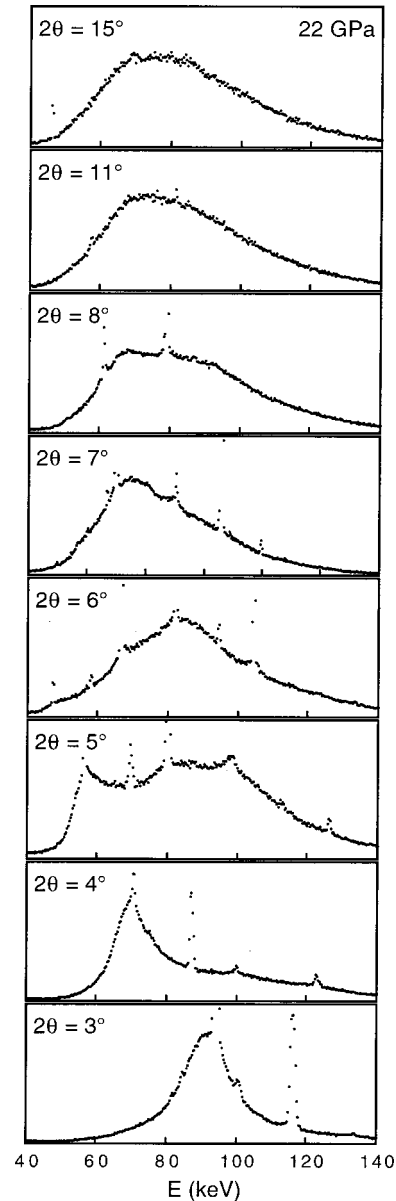


FIG. 2. An example of x-ray-diffraction profiles of *l*-Te, measured at 22 GPa. Sharp peaks are diffraction lines of NaCl (Fig. 1). Data at $60 \leq E \leq 120$ keV, where E is x-ray energy, were used for analyses.

GPa.^{14,17,22,27} The total x-ray counts used to determine each $S(Q)$ were approximately 4×10^6 .

III. RESULTS AND DISCUSSION

Pressure dependence of $S(Q)$ [Fig. 4(a)] provides overall information on the structural transformation. The first and the second peaks of $S(Q)$ are key features representing the interchain coupling and intrachain covalent bond, respectively.^{17,22} Collapse of the chain structure, associated with enhancement of interchain interaction, is inferred from peak-height changes; the first peak grows and the second diminishes with pressure. Drastic decrease in interchain distance is inferred from a large shift of the first-peak position toward higher Q values. With increasing pressure, it becomes

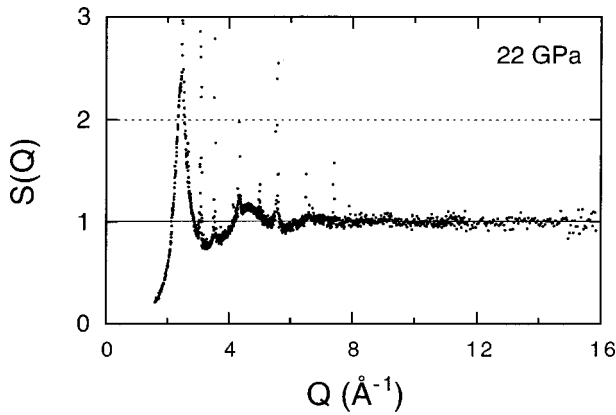


FIG. 3. An example of static structure factor $S(Q)$ of l -Te, measured at 22 GPa. Sharp peaks are diffraction lines of NaCl (Fig. 1).

difficult to observe the oscillation of $S(Q)$ at a high- Q range (Fig. 3), probably due to the collapse of covalency, resulting in a broadening of the first peak of $g(r)$ [Fig. 4(b)]. The $S(Q)$ at 22 GPa is almost similar to those of simple liquids. However, a trace of the second peak indicates that the structure cannot be fully explained as a simple liquid.

Detailed structural transformation can be discussed based on $g(r)$ [Fig. 4(b)]. The atoms just outside the first coordination shell (i.e., $3.4 \leq r \leq 4.8 \text{ \AA}$) move toward the nearest-neighbor distance with increasing pressure, consistent with the inference from the variations in $S(Q)$. This corresponds to the enhancement of the interchain coupling and may result in the weakening of the intrachain covalent bond, as inferred from the anomalous behavior of r_1 (Fig. 5). In spite of the volume contraction, r_1 increases from 2.9–3.0 \AA at 0 GPa^{14,17,22,27} to 3.1 \AA at 6 GPa. Above 6 GPa, r_1 decreases

gradually with pressure but not as much as expected from uniform contraction with $d(r_1/r_{1(P=0)})/d([V/V_{(P=0)}]^{1/3}) = 1$, which is characteristic of simple liquids.¹³

In c -Te, Te (I) with a twofold coordinated spiral-chain structure (Se type) transforms to Te (II) with a fourfold puckered-layer structure at 4 GPa and 300 K.¹⁸ The $g(r)$ at 6 GPa is as expected from the bond-length distribution of Te (II) (Fig. 6). Integration of $4\pi\rho r^2 g(r) dr$ from distance $r = 2.20 \text{ \AA}$ to $r = 3.25, 3.80, \text{ and } 5.15 \text{ \AA}$ gives 4.1, 8.0, and 18.4 atoms, respectively, providing additional validation [see the numbers for Te (II) in Fig. 6]. At 300 K, Te (II) further transforms to Te (III) at 7 GPa just changing the symmetry from monoclinic to orthorhombic,^{2,18} then to Te (IV) with the sixfold rhombohedrally distorted simple cubic structure (β -Po type) at 10 GPa,^{2,19} and finally to Te (V) with the eightfold body-centered-cubic (bcc) structure at 27 GPa.² Only small displacements of atomic positions are required throughout Te (II) to Te (V) transformations.³ This may correspond to the mild structural changes observed in l -Te above 6 GPa. The $g(r)$ at 22 GPa is almost as expected from Te (V), i.e., a simple liquid with a coordination number of 14 (8 plus 6) (Fig. 6). Indeed, the coordination number obtained from integration of $4\pi\rho r^2 g(r) dr$ up to $r = 4.35 \text{ \AA}$ [the first minimum of $g(r)$] is 13.6. However, as discussed above, the structure cannot be explained as the simple liquid. The transformation will be completed at a higher pressure.

Based on the present results, l -Te may have a fourfold structure at 6 GPa. The similarity between supercooled l -Te and the twofold Te (I) has been suggested from both diffraction and extended x-ray-absorption fine-structure (EXAFS) studies at 0 GPa.^{14,16,17} Therefore the intermediate liquid phase with a stability field between two reported transitions at 0 and 5 GPa most likely has a coordination number of

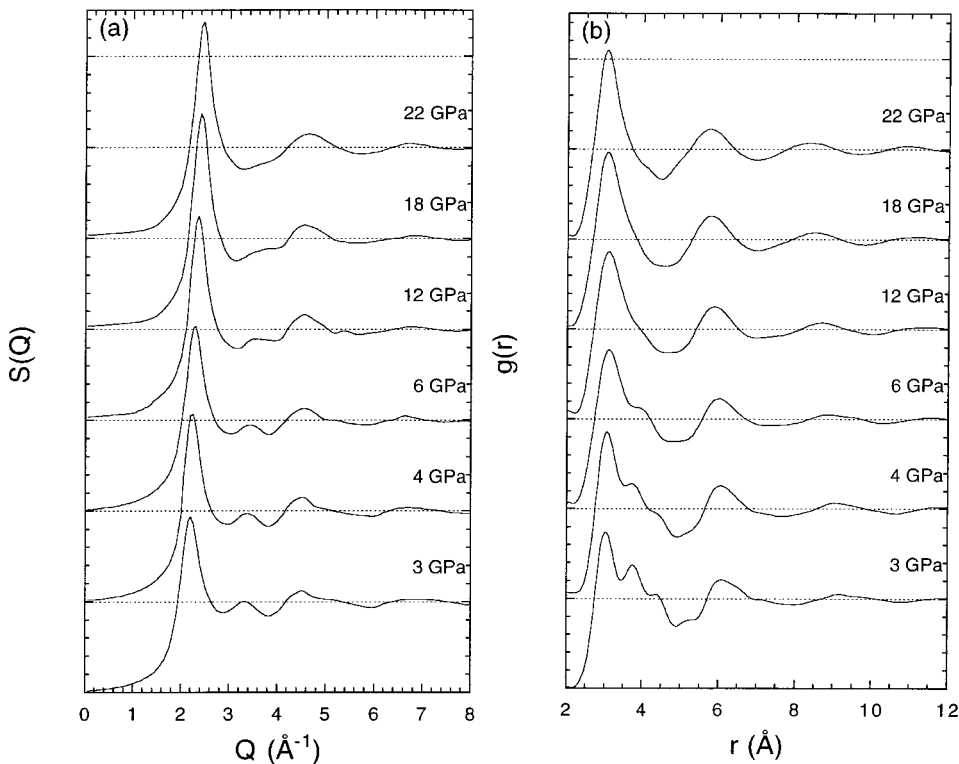


FIG. 4. Variations of local structure in l -Te with pressure. (a) Static structure factor $S(Q)$ and (b) pair distribution function $g(r)$. Horizontal lines are drawn every one unit for $S(Q)$ and $g(r)$.

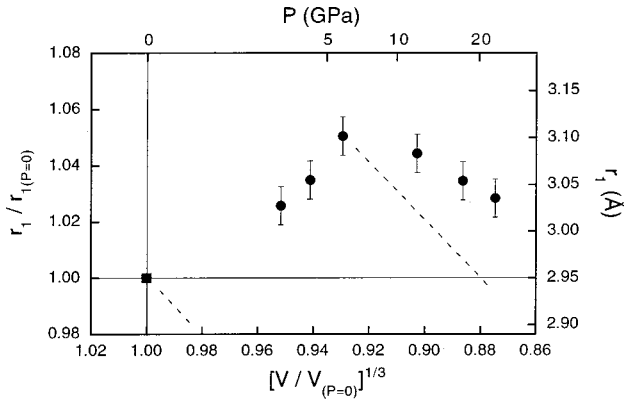


FIG. 5. Volume dependence of the nearest-neighbor distance r_1 of l -Te. The 0-GPa data are taken from previous work (Refs. 14, 17, 22, and 27). Note that r_1 of c -Te (I) is 2.8 Å at 0 GPa (Ref. 28). Dashed lines represent hypothetical variations of r_1 based on the uniform contraction model (see text).

about 3. Because of the complicated shapes of $g(r)$, however, it is almost impossible to determine the exact coordination number at 3 and 4 GPa. Here, we just point out that the integration of $4\pi r^2 g(r) dr$ from $r=2.20$ Å to $r=3.25$ Å gives smaller numbers at 3 and 4 GPa (3.5 and 3.8 atoms, respectively) than the number at 6 GPa (4.1 atoms).

The EXAFS studies at 0 GPa have demonstrated that r_1 is 2.8 Å (short bond) in the semiconducting state while 3.0 Å (long bond) appears in the metallic state in addition to 2.8 Å.^{16,17} As the two bonds cannot be resolved and, furthermore, as peak positions are affected by the second-neighbor bonds, r_1 reported from diffraction studies at 0 GPa ranged from 2.9 to 3.0 Å,^{14,17,22,27} although the precision of r_1 is typically ± 0.01 Å. Our results of r_1 may not be ideal for the same reasons. Nevertheless, we emphasize that r_1 of 3.1 Å at 6 GPa is consistent with the fourfold Te (II) (Fig. 6). Since 2.8 Å is related with the twofold Te (I),²⁸ we believe, 3.0 Å in the metallic state may be originated from a threefold structure. The r_1 at 3 and 4 GPa, where we suppose the predominance of a threefold structure, are rather close to 3.0 Å (Fig. 5). Most of the diffraction studies at 0 GPa have suggested that the coordination number of the metallic phase is close to 3.^{14,27} The occurrence of a threefold structure is also supported by a tight-binding Monte Carlo simulation.²⁰

Our basic idea is that the predominant structure of l -Te is threefold between 0 and 5 GPa. However, the increases in both r_1 and the number of atoms inside a given distance (e.g., 3.25 Å) indicate that increasing pressure may promote the transformation from two- to three- and then to fourfold structures over this pressure range. The continuous transformation is consistent with the rapid increase in electrical conductivity with pressure measured up to 1 GPa,²⁹ and the occurrence of a melting temperature maximum found at 1 GPa,^{7,30} which corresponds to the drastic volume contraction with pressure.

Precision of r_1 determination may be worth discussion. In the present study, we used two systems, SPEED-1500 for 6-, 12-, 18-, and 22-GPa measurements and MAX90 for 3- and 4-GPa measurements. We have used these two systems also for group-IV liquids, l -Si and l -Ge, so far,³¹ and have con-

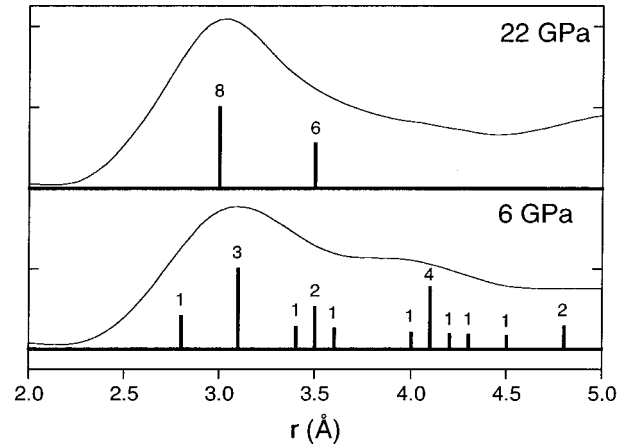


FIG. 6. Comparison of structures between l - and c -Te phases under pressure. Magnified view of pair distribution function $g(r)$ of l -Te at 6 and 22 GPa (curves) is shown together with bond-length distribution of c -Te (II) at 5 GPa (Ref. 18) and c -Te (V) at 30 GPa (Ref. 2) (bars), respectively. For c -Te, number of atoms at distance r , which is labeled on the bars, is divided by r^2 and then normalized by the maximum value for each phase. Ticks on vertical axis are drawn every one unit.

firmed that any systematic errors in r_1 , due to the differences in experimental setup, are not detectable. During data processing, we made minor corrections to get $S(Q)$ and $g(r)$ consistent with each other and physically appropriate, as discussed above. We have examined the effects of the corrections, and have confirmed that the r_1 obtained with the corrections is identical to the r_1 without the corrections well within ± 0.01 Å. Finally, we have checked the effects of finite truncation of Fourier transformation. The truncation of $S(Q)$ at a smaller Q value than 16 Å⁻¹ (the maximum Q value of the present study) resulted in a slightly larger r_1 than shown in Fig. 5. However, even for 3-GPa data, in which the oscillation of $S(Q)$ is relatively large at a high- Q range, the truncation at 8 Å⁻¹ affected r_1 by only 0.02 Å. For 22-GPa data, the truncation at the same Q value affected r_1 by 0.01 Å. Therefore we estimate that the precision of the present study is better than ± 0.02 Å (the error bars in Fig. 5).

In highly anisotropic covalent state at low pressures, l -Te contracts with pressure mainly by increasing the coordination number and reducing the anisotropy. When the second- and higher-neighbor atoms approach, the electron distribution around the atom shifts toward these directions. This results in the weakening of the covalent bond and hence the expansion of r_1 observed below 6 GPa. However, in less anisotropic metallic state at high pressures, the difference in the strength of each bond is small and therefore l -Te cannot contract effectively any longer by the same mechanism. As a result, r_1 decreases with pressure above 6 GPa, but still not as much as expected from uniform contraction because of the residual anisotropy. The effect of pressure on the structure of l -Te is much smaller in a dense metallic state at high pressures than in a sparse covalent state at low pressures.

The formation of long-lived crystal-like clusters may play an important role in the two transitions of l -Te.⁷ Generally, destruction and reconstruction of bonding occurs frequently

and constituent atoms do not have any fixed coordination numbers in the liquid state. In *l*-Te at relatively low pressures, however, an average coordination number is rather small and the bonding has a covalent nature. This covalency may stabilize the clusters mainly consisting of two-, three-, and fourfold atoms with increasing pressure. Probably because of the formation of the threefold cluster, the transition pressure to a fourfold structure is higher in *l*-Te than in *c*-Te (5 and 4 GPa, respectively), which transforms to fourfold directly from twofold. The bonding becomes more metallic with pressure. Delocalized electrons enhance the destruction and reconstruction of bonding, so that the formation of clusters becomes more difficult. Gradual transformation at high pressures may be largely due to the highly metallic nature of bonding.

IV. CONCLUSION

Our experimental techniques made it possible to study the structure of liquids at extreme high-pressure conditions. The advance of experimental techniques must motivate theoretic-

cal calculations for liquids at high pressures and high temperatures, as the validity of calculations can be evaluated using experimental results or theoretical predications can be proved by experiments.

Using these techniques, we have clarified similarities and differences in pressure-induced structural changes between *l*- and *c*-Te up to above 20 GPa. Continuous structural changes and the presence of a threefold structure are characteristic of *l*-Te. Anomalous pressure dependence of r_1 is found in *l*-Te; r_1 expands against compression in sparse covalent state and it contracts in dense metallic state at higher pressures.

ACKNOWLEDGMENTS

We thank K. Funakoshi, W. Utsumi, T. Kikegawa, S. Urakawa, M. Imai, N. Nishiyama, T. Yagi, T. Uchida, T. Sumita, M. Ohtani, N. Hosokawa, and T. Mori for experimental support. Synchrotron x-ray-diffraction experiments were carried out at SPring-8 and PF using SPEED-1500 and MAX90 systems.

-
- *Present address: Department of Earth and Planetary Science, University of Tokyo, Tokyo 113-0033, Japan.
- ¹R. Keller, W. B. Holzapfel, and H. Schulz, *Phys. Rev. B* **16**, 4404 (1977); O. Shimomura, K. Takemura, Y. Fujii, S. Minomura, M. Mori, Y. Noda, and Y. Yamada, *ibid.* **18**, 715 (1978).
 - ²G. Parthasarathy and W. B. Holzapfel, *Phys. Rev. B* **37**, 8499 (1988).
 - ³Y. Akahama, M. Kobayashi, and H. Kawamura, *Phys. Rev. B* **47**, 20 (1993).
 - ⁴Y. Fujii, K. Hase, N. Hamaya, Y. Ohishi, A. Onodera, O. Shimomura, and K. Takemura, *Phys. Rev. Lett.* **58**, 796 (1987).
 - ⁵K. Tsuji, *J. Non-Cryst. Solids* **117-118**, 27 (1990).
 - ⁶E. Rapoport, *J. Chem. Phys.* **46**, 2891 (1967).
 - ⁷V. V. Brazhkin, R. N. Voloshin, S. V. Popova, and A. G. Umnov, *J. Phys.: Condens. Matter* **4**, 1419 (1992).
 - ⁸V. V. Brazhkin, R. N. Voloshin, and S. V. Popova, *JETP Lett.* **50**, 424 (1989).
 - ⁹Y. Katayama, T. Mizutani, W. Utsumi, O. Shimomura, M. Yamakata, and K. Funakoshi, *Nature (London)* **403**, 170 (2000).
 - ¹⁰D. A. Young, *Phase Diagrams of the Elements* (University of California Press, Berkeley, 1991); L. Liu and W. A. Basset, *Elements, Oxides, Silicates* (Oxford University Press, New York, 1986).
 - ¹¹K. Tsuji, K. Yaoita, M. Imai, O. Shimomura, and T. Kikegawa, *Rev. Sci. Instrum.* **60**, 2425 (1989).
 - ¹²K. Yaoita, K. Tsuji, Y. Katayama, N. Koyama, T. Kikegawa, and O. Shimomura, *J. Non-Cryst. Solids* **156-158**, 157 (1993).
 - ¹³K. Tsuji, Y. Katayama, Y. Morimoto, and O. Shimomura, *J. Non-Cryst. Solids* **205-207**, 295 (1996).
 - ¹⁴A. Menelle, R. Bellissent, and A. M. Flank, *Europhys. Lett.* **4**, 705 (1987); *Physica B* **156-157**, 174 (1989).
 - ¹⁵H. Thurn and J. Ruska, *J. Non-Cryst. Solids* **22**, 331 (1976).
 - ¹⁶K. Tamura, M. Inui, M. Yao, H. Endo, S. Hosokawa, H. Hoshino, Y. Katayama, and K. Maruyama, *J. Phys.: Condens. Matter* **3**, 7495 (1991).
 - ¹⁷T. Tsuzuki, M. Yao, and H. Endo, *J. Phys. Soc. Jpn.* **64**, 485 (1995).
 - ¹⁸K. Aoki, O. Shimomura, and S. Minomura, *J. Phys. Soc. Jpn.* **48**, 551 (1980).
 - ¹⁹J. C. Jamieson and D. B. McWhan, *J. Chem. Phys.* **43**, 1149 (1965).
 - ²⁰C. Bichara, J.-Y. Raty, and J.-P. Gaspard, *Phys. Rev. B* **53**, 206 (1995).
 - ²¹W. W. Warren, Jr. and R. Dupree, *Phys. Rev. B* **22**, 2257 (1980); M. Misonou and H. Endo, *J. Phys. Soc. Jpn.* **51**, 2285 (1982); J. Hafner, *J. Phys.: Condens. Matter* **2**, 1271 (1990); K. Tamura, *J. Non-Cryst. Solids* **205-207**, 239 (1996).
 - ²²M. Misawa, *J. Phys.: Condens. Matter* **4**, 9491 (1992).
 - ²³Y. Katayama, K. Tsuji, H. Kanda, H. Nosaka, K. Yaoita, T. Kikegawa, and O. Shimomura, *J. Non-Cryst. Solids* **205-207**, 451 (1996).
 - ²⁴See, for example, T. Irifune *et al.*, *Science* **279**, 1698 (1998). MA8-type anvils made of cemented tungsten carbide with a truncated-edge length (TEL) of 3.5 mm were used in the highest-pressure measurement at 22 GPa; otherwise, the anvils with a TEL of 5.0 mm were used.
 - ²⁵D. L. Decker, *J. Appl. Phys.* **42**, 3239 (1971).
 - ²⁶Number densities ρ used in the Fourier transformations are 0.032, 0.033, 0.035, 0.038, 0.040, and 0.041 \AA^{-3} at 3, 4, 6, 12, 18, and 22 GPa, respectively.
 - ²⁷G. Tourand and M. Breuil, *J. Phys. (France)* **32**, 813 (1971); W. Hoyer, E. Thomas, and M. Wobst, *Z. Naturforsch. A* **30A**, 235 (1975); Y. Waseda and S. Tamaki, *Z. Naturforsch. A* **30A**, 1655 (1975); S. Takeda, S. Tamaki, and Y. Waseda, *J. Phys. Soc. Jpn.* **53**, 3830 (1984).
 - ²⁸C. Adenis, V. Langer, and O. Lindqvist, *Acta Crystallogr., Sect. C: Cryst. Struct. Commun.* **C45**, 941 (1989).
 - ²⁹K. Tamura, M. Misonou, and H. Endo, *J. Phys. Soc. Jpn.* **46**, 637 (1979).
 - ³⁰P. E. Chaney and S. E. Babb, Jr., *J. Chem. Phys.* **43**, 1071 (1965); S. M. Stishov, N. A. Tikhomirova, and E. Yu. Tonkov, *JETP Lett.* **4**, 111 (1966).
 - ³¹N. Funamori and K. Tsuji (unpublished).